High-Density Helicon Plasma Thrusters using Electrodeless Acceleration Schemes

IEPC-2015-386／ISTS-2015-b-386

Presented at Joint Conference of 30th International Symposium on Space Technology and Science 34th International Electric Propulsion Conference and 6th Nano-satellite Symposium, Hyogo-Kobe, Japan July 4 – 10, 2015

Daisuke Kuwahara[1], Shunjiro Shinohara[2], Takamichi Ishii[3], Shuhei Otsuka[4], Toshiki Nakagawa[5], Kensuke Kishi[6], Marie Sakata[7], Eiko Tanaka[8], Hiraku Iwaya[9], Kohei Takizawa[10], Yuriko Tanida[11], Takayuki Naito[12], Kazuki Yano[13], Takahiro Nakamura[14], Sho Ito[15], and Hiroyuki Nishida[16]
Tokyo University of technology, Koganei, Tokyo, 184-8550, Japan

Abstract: We have been studying long-lifetime helicon plasma thrusters as the Helicon Electrodeless Advanced Thruster (HEAT) project. Two important elements of the proposed helicon plasma thruster are a generation of a dense source plasma using a helicon wave, and an acceleration of the plasma by the Lorentz force using the product of the induced azimuthal current and static radial magnetic field. Here, in order to eliminate damage of electrodes, both generation and acceleration schemes are operated in non-contact condition between the plasma and electrodes. Acceleration schemes use two type of coils: rotating magnetic field coils and azimuthal mode number *m* = 0 ones. These studies have been carried out mostly on the Large Mirror Device (LMD), which has two types the magnetic field source, permanent magnets and electromagnets. To verify our acceleration schemes, LMD can accept various diagnostics using a direct and an indirect (optical) measurements. In this paper, current performances of generation and acceleration schemes and the thrust measurement system are reported.

Nomenclature

B	=	applied field strength [G]
B_r	=	radial component of magnetic field [G]
B_ω	=	rotating magnetic field [G]
e	=	elementary charge [C]
E_z	=	axial component of electric field [V/m]
F	=	thrust [mN]
f_{ce}	=	electron cyclotron frequency [Hz]
f_{ci}	=	ion cyclotron frequency [Hz]
$f_{m=0}$	=	frequency of $m = 0$ coil current [Hz]
FR	=	gas flow rate [sccm]
f_{RF}	=	excitation frequency [Hz]
f_{RMF}	=	frequency of rotating magnetic field [Hz]
F_z	=	axial component of Lorentz force [N]
$I_{m=0}$	=	current of $m = 0$ coil [A]
I_{RMF}	=	current of RMF coil [A]
I_{sp}	=	specific impulse [s]
j_θ	=	azimuthal component of induced current density [A/m^2]
j_z	=	axial component of induced current density[A/m^2]
n_e	=	electron density [m^{-3}]
n_i	=	ion density [m^{-3}]

n_0	=	neutral particle density [m^{-3}]
P	=	filling pressure [Pa]
P_{RF}	=	Radio frequency power [W]
r	=	radial position [mm]
T_e	=	electron temperature [eV]
$v_{e\theta}$	=	electron flow velocity [m/s]
v_i	=	ion flow velocity [m/s]
z	=	axial position [mm]
η_P	=	thrust to power ratio [mN/kW]

[1]Assistant Professor, Department of Mechanical System Engineering, dkuwahar@cc.tuat.ac.jp
[2]Proffessor, Department of Mechanical System Engineering, sshinoha@cc.tuat.ac.jp
[3]Graduate Student, Department of Mechanical System Engineering, ishii.iiishi.7@gmail.com
[4]Graduate Student, Department of Mechanical System Engineering, so.50013643016@gmail.com
[5]Graduate Student, Department of Mechanical System Engineering, yukasenzai@gmail.com
[6]Graduate Student, Department of Mechanical System Engineering, 50014643021@st.tuat.ac.jp
[7]Graduate Student, Department of Management of Technology, 50014648117@st.tuat.ac.jp
[8]Graduate Student, Department of Mechanical System Engineering, 50014643044@st.tuat.ac.jp
[9]Graduate Student, Department of Management of Technology, 50015648107@st.tuat.ac.jp
[10]Graduate Student, Department of Mechanical System Engineering, 50015643038@st.tuat.ac.jp
[11]Graduate Student, Department of Mechanical System Engineering, 50015643041@st.tuat.ac.jp
[12]Graduate Student, Department of Mechanical System Engineering, 50015643048@st.tuat.ac.jp
[13]Graduate Student, Department of Mechanical System Engineering, 50015643071@st.tuat.ac.jp
[14]Ph.D., Department of Mechanical System Engineering, takahiro.nakamura1@gmail.com
[15]Graduate Student, Department of Mechanical System Engineering, 50014643009@st.tuat.ac.jp
[16]Associate Professor, Department of Mechanical System Engineering, hnishida@cc.tuat.ac.jp

I. Introduction

MOST practical electric thrusters have a lifetime problem coming from a damage of electrodes directly contacting with a plasma. A helicon plasma thruster is proposed as a long-lifetime electric thruster which has non-direct contact electrodes. This thruster works without any contact electrodes, therefore it has a potential to become a long-lifetime and high-thrust propulsion system, such as a main thruster for a deep space explorer. Development of the helicon plasma thruster has been conducted under the Helicon Electrodeless Advanced Thruster (HEAT) project, in which no electrodes contact with the plasma directly[1].

First, we generate a dense source plasma using a helicon wave with an excitation frequency between an ion and an electron cyclotron frequencies, f_{ci} and f_{ce}, respectively applied from the outside of a discharge using a radio frequency (RF) antenna. The helicon plasma is known as a high-density (~10^{19} m^{-3}), a high-ionization ratio (of up to several tens of percent), and a high particle generation efficiency discharge method[2]. In addition, its operational ranges are wide and flexible, such as an applied magnetic field B, a fill pressure P and an RF frequency f_{RF}. Second, in order to achieve high thrust and specific impulse, we accelerate the dense plasma source by the axial Lorentz force F_z using the product of the induced azimuthal current j_θ and the static radial magnetic field B_r, shown in Eq. (1).

$$f_z = j_\theta \times B_r \,. \tag{1}$$

There are several methods proposed in our HEAT project for exciting j_θ in the plasma, and our laboratory has been developing schemes that use two types of coils: rotating magnetic fled (RMF) coils[1,3] and an azimuthal mode number m = 0 coil[1,4,5]. Here, B_r is generated using a combination of permanent magnets, which has relatively large B_r component, and electromagnets surrounding a discharge tube to generate the axial field mainly.

To develop these schemes, an estimation of propulsion efficiencies, such as a plasma thrust, a specific impulse and a thrust efficiency, is necessary. In order to measure the thrust, a pendulum-type target stand with a cylindrical target has been developed[6]. The target type thrust stand is a good solution for measuring the thrust of a large-diameter, complex and heavy system such as our experimental device, Large Mirror Device (LMD)[7]. LMD can accept many diagnostics, such as electrostatic probes (to measure n_e, T_e, and v_i), spectrometers (gas species, n_e, T_e, and v_i), laser induced fluorescence (v_i and relative n_i), and high-speed camera (plasma plume, relative n_e and n_0). Since various plasma parameters can be derived in this device, we can estimate generation and acceleration schemes in detail[1,8,9].

II. Theory

A. Generation of the helicon plasma

Figure 1 shows a schematic diagram of the helicon plasma thruster. The magnetic field by permanent magnets and electromagnets (only electromagnets are used in Fig. 1 case) is applied in a generation and an acceleration region. In the generation region, the magnetic field is nearly uniform, but on the other hand, in the acceleration region, there is a strong divergent field (large B_r) having a larger thrust in the presence of j_θ. Inside of a discharge tube, made of a quartz, is filled with a propellant gas (argon and xenon). RF power is fed to the propellant gas via an RF antenna, wound on the outer surface of the discharge tube, thus, the high-density helicon plasma is generated.

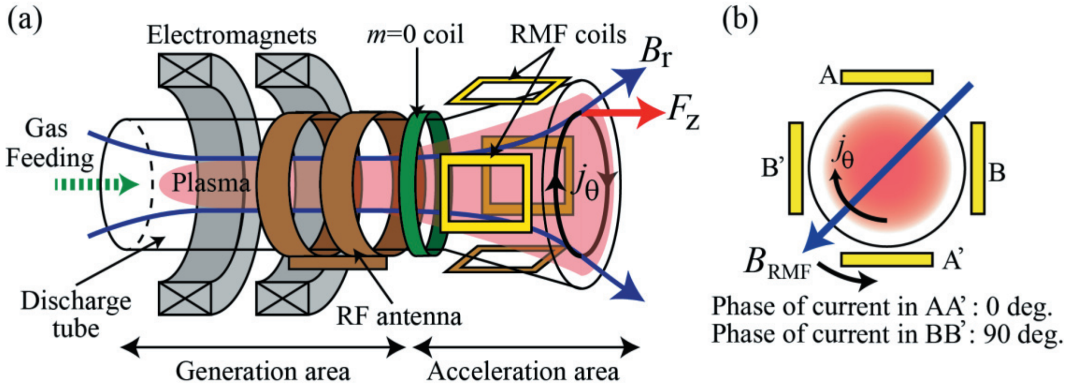

Fig. 1 Schematics of helicon plasma thruster: (a) side view, and (b) cross-sectional view of RMF coils (90 deg. Phase difference).

B. Acceleration: RMF coils method

The RMF scheme was originally developed as a concept to maintain the Field Reversed Configuration (FRC) in a magnetically confined fusion research[3]. Here, RMF coils are exerted to generate j_θ, as shown in Fig. 1. First, the rotating magnetic field B_ω is generated by two pairs of RMF coils with AC currents, which have a phase difference of 90 degrees between the pairs. Due to the Faraday's law, an axial electric field $\widetilde{E_z}$ is induced. Second, an axial current $\widetilde{j_\theta}$ is generated by the effects of electron-ion collision an electron-neutral collision through the Ohm's law. Third, the azimuthal electric field is generated by the nonlinear term of $\widetilde{j_z} \cdot \widetilde{B_r}$ ($\widetilde{B_r}$ is radial AC component of B_ω), and the retarding torque generated by the collision effects again. Azimuthal current j_θ is generated as Eq. (2).

$$j_\theta = -n_e er \cdot 2\pi f_{RMF} . \quad (2)$$

Finally, the axial Lorentz force f_z for plasma acceleration is generated as Eq. (1). Here, j_θ is proportional to n_e and f_{RMF}, when B_ω is penetrated into the plasma completely.

C. Acceleration: *m* = 0 coil method

m = 0 coil is shown in Figure 1(a), located in the acceleration region. In this scheme, the *m* = 0 coil applied with AC current ($f_{m=0}$ < 100 kHz) generates an alternating axial magnetic field, which induces alternating j_θ, therefore, this scheme behaves like a transformer. This acceleration method is a half cycle acceleration; the acceleration and deceleration phases. However, the momentum generated in the deceleration phase is canceled due to the collision to the wall of the discharge tube. One of problems is a penetration of the alternating magnetic field into the plasma, same as the RMF scheme. Important operating parameters to achieve the thrust, are the radial component of static magnetic field strength B_r, a frequency of the *m* = 0 coil current $f_{m=0}$, and magneto motive force of *m* = 0 coil[1,5].

III. Experiment

A. RMF coils acceleration experiment

Figure 2 shows an experimental setup of LMD. A quartz discharge tube [1,000 mm in length and 100 - 170 mm in inner diameter (i.d.)] has a tapered shape to prevent a wall loss of plasmas in a divergent magnetic field area (acceleration area). This tube is connected to a vacuum chamber (1,700 mm in length and 445 mm in i.d.). LMD has two turbo-molecular pumps (1,000 and 2,400 l/s) with a base pressure ~10^{-4} Pa. Argon gas was used as a propellant one, and a typical discharge pressure was > 0.1 Pa. Plasma is generated by a RF power via a half-helical antenna. The RF typical input power P_{RF} and its excitation frequency f_{RF} were ~3 kW and 7 MHz, respectively. There were two types of applied magnetic field system; permanent magnets and electromagnets[10]. In the case of the RMF experiment, only permanent magnets were used. Permanent magnets were placed in the straight section of the quartz tube generate a large magnetic field in the radial direction. Two pairs of RMF coils had 5 turns in each plane (168 × 115 mm). The material of the RMF coils was oxygen-free copper with 15 mm width and 0.5 mm thickness. The distance between the facing coils was 225 mm, and an axial position of the coil center was z = -245 mm, where B_r was large. To check the plasma flow, a Mach probe was used to measure n_e and v_i, employing the unmagnetized model (model constant κ = 1.26)[11].

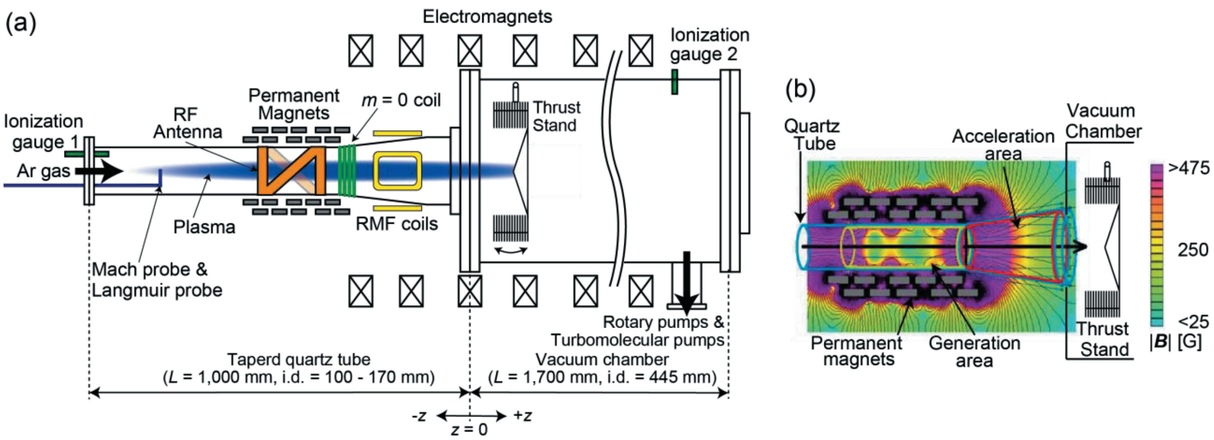

Fig. 2 Experimental setup of LMD: (a) LMD, and (b) magnetic field profile generated by permanent magnets[7-10].

Figure 3 indicates v_i and n_e, changing RMF coil current I_{RMF} and gas flow rate FR. In this experiments, P_{RF} and measurement point are 1,000 W and z = -130 mm with r = 60 mm, respectively. Two types of phase difference between RMF coil current were tested; 90 deg. (acceleration phase) and -90 deg. (deceleration phase). The range of I_{RMF} was 0 - 30 A in the previous research[12], which was increased to 50 A in the present experiment. In the cases of acceleration phase, v_i and n_e were increased by increasing I_{RMF}. However, in the cases of deceleration phase, v_i and n_e were almost unchanged. These results indicate that the RMF acceleration scheme is promising. The maximum increasing rates of v_i and n_e were ~19 % and ~29 %, respectively, in the case of I_{RMF} = 50 A and FR = 40 sccm. As is shown in Fig. 3, the acceleration effect was increased in the case of low gas flow rate, which comes from the low electron-neutral collision frequency.

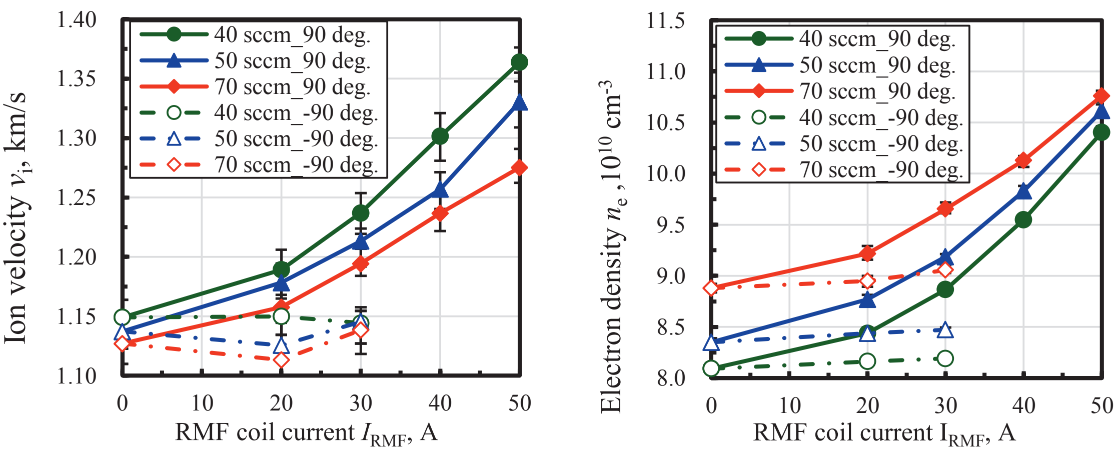

Fig. 3 RMF acceleration effects, i.e., v_i and n_e vs. I_{RMF} and FR (P_{RF} = 1,000 W, z = -130 mm, and r = 60 mm).

B. *m* = 0 coil acceleration experiment

To verify the $m = 0$ coil acceleration scheme, we have carried out the experiments using the Small Helicon Device (SHD)[13-15]. Figure 4(a) shows a side view of this device, which consists of 4 parts, i.e., a gas feeding system, a discharge tube, a vacuum chamber and vacuum pumps. The discharge tube is made of a quartz tube, 20 mm i.d. with an axial length of 453 mm. The vacuum chamber is made of a SUS316 pipe, 165 mm i.d., and 865 mm with an axial length, works as a buffer tank. An electromagnet installed in the discharge tube region generates an axial magnetic field component for generating a source plasma, and a radial component for accelerating the plasma. An RF antenna, installed in a upstream region relative to the electromagnet, transfers RF power up to 2 kW with a frequency of 7 MHz. An $m = 0$ coil is installed in the downstream region of the electromagnet, where the radial field component is large. The detail of the setup in the source region (acceleration region) is indicated in Fig. 4(b).

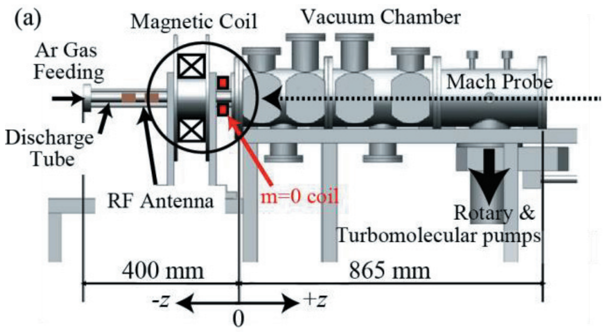

Fig. 4 Experimental setup of SHD: (a) Side view of SHD, and (b) acceleration region[13-15]

Figure 5 shows a preliminary result of the $m = 0$ coil experiment. Red and blue solid lines indicate ion velocities with and without $m = 0$ coil acceleration, respectively. Each ion velocity is measured by the Mach probe at the position of $z = -25$ mm with $r = 0$ and 6 mm. A green dotted line indicates the current of $m = 0$ coil. From the principle, the ion velocity is expected to be accelerated and decelerated alternatively, like the case of $r = 0$ mm. However, in the case of $r = 6$ mm, v_i was accelerating in both accelerating and decelerating phases of $I_{m=0}$, like a wave form of a full wave rectification. In this experiment, a changing of an electron density was small. From these results, we considered that the $m = 0$ coil acceleration was dominant near the central region of the plasma (around $r = 0$), and the Ponderomotive force was also important in the outer edge region of the plasma[16-18].

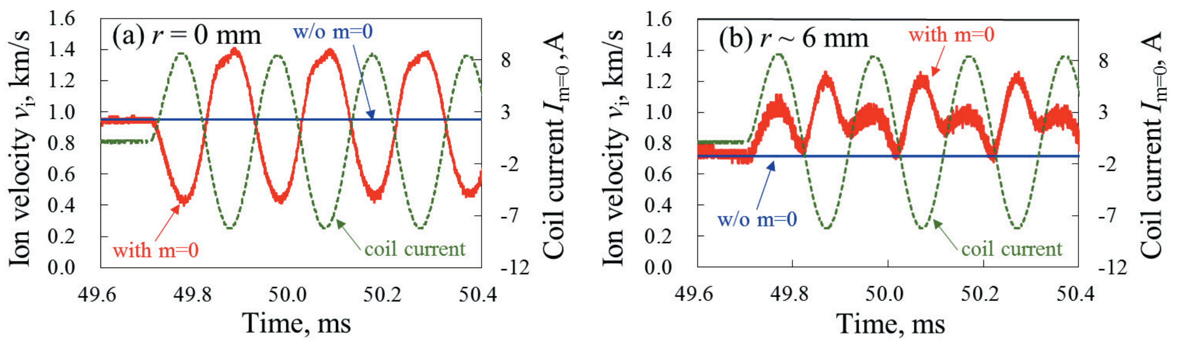

Fig. 5 Experimental result of m = 0 coil acceleration: (a) $r = 0$ mm, and (b) $r \sim 6$ mm.

C. Direct Thrust measurement of the source dense plasma

In this section, thrust characteristics of the source dense plasma generated by permanent magnets and electromagnet on LMD are presented. Figure 6 shows the cylindrical target type thrust stand installed in LMD[6]. This thrust stand was installed in front of the open end of the discharge tube, $z = 20$ mm (see Fig. 2). The cylindrical target consists of a corn-shape end plate with a 60 degree span from the plasma axis in outer diameter (o.d.) of 320 mm, and of a series of 14 disks, 240 mm i.d. and 320 mm o.d. with a thickness of 1 mm. The distance between neighboring disks and the end plate is 9 mm. Produced ions and neutral particles ejected from the quartz tube enter the target, then collide and reflect by the corn-shape end plate, and reflected particles enter gap regions of disks. Since particles collide with disks many times, they transfer their axial momentum mv (m: particle mass, v: axial velocity) to the target (inelastic condition). The material of the end plate and disks are SUS316 and polycarbonate, respectively. An impulse bit is measuring by the displacement of the target using a laser displacement sensor. A thrust is calculated by the impulse bit and the discharge duration.

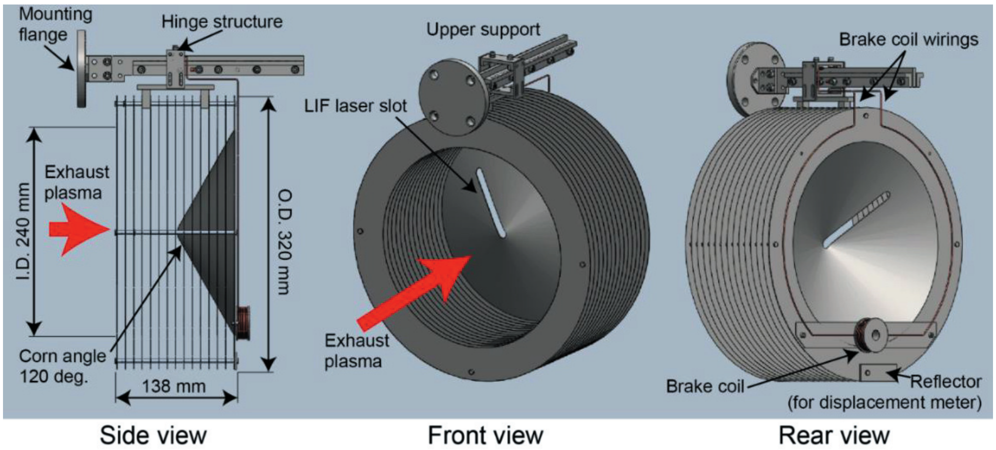

Fig. 6 Cylindrical target on LMD[6] (ring: polycarbonate, corn: SUS314).

Figures 7 and 8 indicate experimental results of Ar and Xe discharges, respectively. Thrust F, thrust to power ratio η_P, i.e., F/P_{RF}, and specific impulse I_{sp} were measured under various P_{RF}, FR, and current of electromagnets I. The largest values of F, η_P, and I_{sp} of Ar (Xe) discharge independently obtained, were 21 (41) mN, 8.3 (16) mN/kW, and 2,000 (1,500) s, respectively. The thrust showed an increased tendency with P_{RF}, FR, and I. However, η_P were decreased with P_{RF}. For I_{sp}, the largest value was observed in large P_{RF} and small FR and I. These parameters also show promising plasma performance in spite of no active acceleration schemes. Furthermore, improving these values by applying the acceleration proposed can be expected.

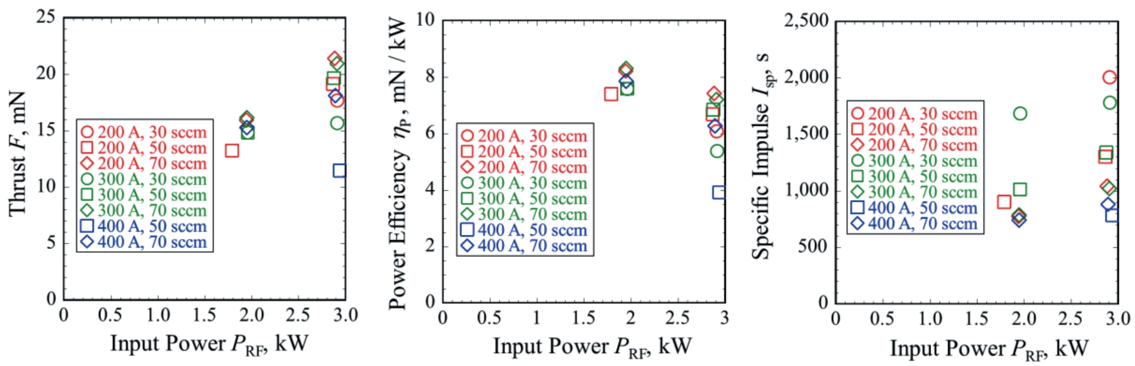

Fig. 7 Thrust performance in Ar discharges.

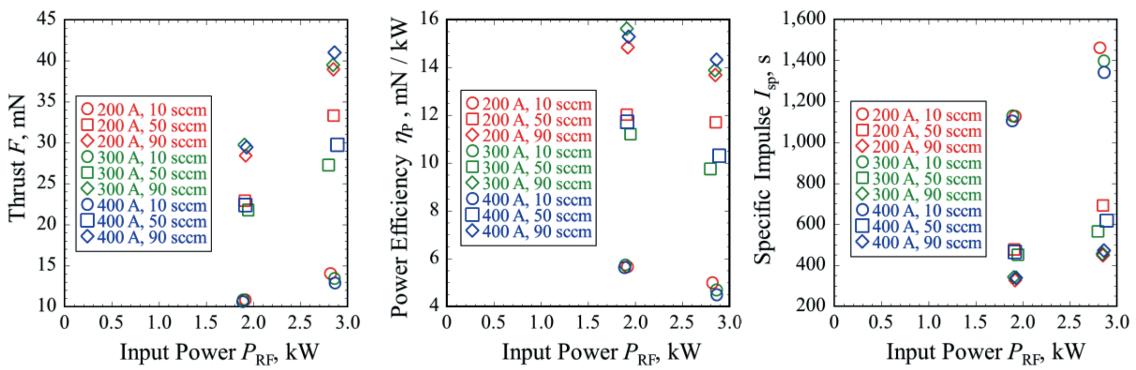

Fig. 8 Thrust performance in Xe discharges.

To verify an accuracy of the present cylindrical target type thrust stand, thrust values were compared with another type thrust stand. Figure 9 shows an experimental setup for this comparison. The thruster installed on a torsional type thrust stand was a compact helicon plasma thruster using a strong permanent magnets[19]. The target type thrust stand was arranged in front of the opening of the thruster with a distance of 65 mm. Materials of the cylindrical target was polycarbonate. Here, all devices were installed in a vacuum chamber. Experimental results showed that observed thrusts of the target stand were smaller than the thrust balance ones by about 20%. The reason of small value is considered that the cylindrical target did not collect whole particles. However, it was clear that the target stand measurement has an enough accuracy to estimate the thrust.

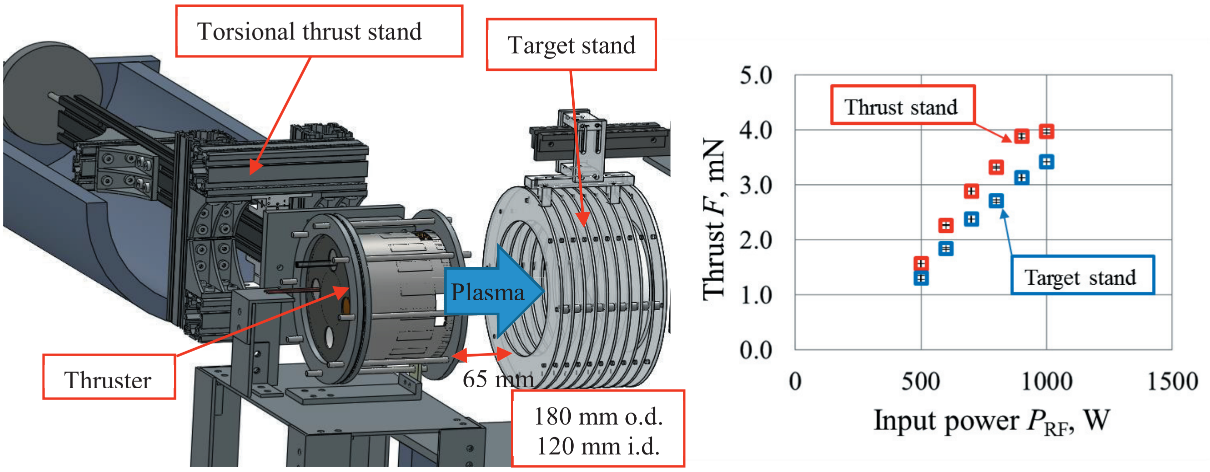

Fig. 9 Experimental of comparison between the torsional thrust stand and the target stand.

IV. Conclusion

In this paper, the generation and acceleration schemes have been investigated separately. In order to study the helicon plasma thruster, especially in the plasma acceleration, we have carried out two proposed types of electromagnetic acceleration schemes. RMF coils scheme has achieved 19 % increase of v_i. The m = 0 coil scheme showed that v_i was increased in both the acceleration and deceleration phases in the outer plasma region. On the other hand, v_i was increased and decreased alternating in the inner plasma region. We considered that these effects were coming from the ponderomotive force and m = 0 acceleration, respectively.

In the case of generating the dense plasma, thrust characteristics were observed using the cylindrical target stand, in Ar and Xe discharges. Largest values F, η_P, and I_{sp} of Ar (Xe) discharge were 21 (41) mN, 8.3 (16) mN/kW, and 2,000 (1,500) s, respectively. In addition, the accuracy of the target stand was checked comparing with the torsional thrust stand.

Acknowledgments

We appreciate the useful discussion with HEAT project members. This research has been supported partially by Grant-in-Aid for Scientific Research (S: 21226019) from the Japan Society for the Promotion of Science.

References

[1]S. Shinohara, H. Nishida, T. Tanikawa, T. Hada, I. Funaki, K. P. Shamrai., "Development of Electrodeless Plasma Thrusters with High-Density Helicon Plasma Sources", *IEEE Trans. Plasma Sci.*, Vol. 42, No. 5, 2014, pp. 1245-1254.

[2]R. W. Boswell, "Plasma Production using a Standing helicon wave", *Phys. Let.*, Vol. 33A, No. 7, 1970, pp. 457-458.

[3]I. R. Jones, "A review of rotating magnetic field current drive and the operation of the rotamak as a field-reversed configuration (Rotamak-FRC) and a spherical tokamak (Rotamak-ST)", *Phys. Plasmas*, Vol. 6, 1999, pp. 1950-1957.

[4]S. Shinohara, T. Hada, T. Motomura, K. Tanaka, T. Tanikawa, K. Toki, Y. Tanaka, K. P. Shamrai, "Development of high-density helicon plasma sources and their applications", *Phys. Plasmas*, Vol. 16, 2009, pp. 057104-1~10.

[5]T. Ishii, H. Ishii, S. Otsuka, N. Teshigahara, H. Fujitsuka, S. Waseda, D. Kuwahara, and S. Shinohara, Study on electrodeless electric propulsion in high-density helicon plasma with permanent magnets", *JPS Conf. Proc.*, Vol. 1, 2014, 015047-1~7.

[6]D. Kuwahara, Y. Koyama, S. Otsuka, T. Ishii, H. Ishii, H. Fujitsuka, S. Waseda, and S. Shinohara, “Development of direct thrust measurement system for the completely electrodeless helicon plasma thruster”, *Plasma Fusion Res.*, Vol. 9, 2014, pp. 3406055-1~4.

[7]S. Shinohara, S. Takechi, Y. Kawai, “Effects of axial magnetic field and Faraday shield on characteristics of RF produced plasma using spiral antenna”, *J. Phys. Soc. Jpn.*, Vol. 35, 1996, pp. 4503-4508.

[8]N. Teshigahara, S. Shinohara, Y. Yamagata, D. Kuwahara and M. Watanabe, “Development of 2D laser induced fluorescence (LIF) system in high-density helicon plasma”, *Plasma Fusion Res.*, Vol. 9, 2014, pp. 3406055-1~4.

[9]S. Waseda, H. Fujitsuka, S. Shinohara, D. Kuwahara, M. Sakata, H. Akatsuka, “Optical measurements of high-density helicon plasma by using a high-speed camera and monochromators”, *Plasma Fusion Res.*, Vol. 9, 2014, pp. 3406125-1~4.

[10]S. Otsuka, T. Nakagawa, H. Ishii, N. Teshigahara, H. Fujitsuka, S. Waseda, T. Ishii, D. Kuwahara, and S. Shinohara, “Generation and acceleration of high-density helicon plasma using permanent magnets for the completely electrodeless propulsion system”, *Plasma Fusion Res.*, Vol. 9, 2014, p. 3406047-1~5.

[11]K. S. Chung, I. H. Hutchinson, B. LaBombard, and R. W. Conn, “Plasma flow measurements along the presheath of a magnetized plasma”, *Phys. Fluids*, Vol. B1, 1989, p. 2229.

[12]S. Otsuka, K. Takizawa, Y. Tanida, D. Kuwahara, and S. Shinohara, “Study on plasma acceleration in completely electrodeless electric propulsion system”, *Plasma Fusion Res.*, Vol. 10, 2015, p. 3401026-1~4.

[13]D. Kuwahara, A. Mishio, T. Nakagawa, and S. Shinohara, “Development of very small-diameter, inductively coupled magnetized plasma device”, *Rev. Sci. Instrum.*, Vol. 84, 2013, pp. 103502-1~4.

[14]T. Nakagawa, S. Shinohara, D. Kuwahara, A. Mishio, and H. Fujitsuka, “Characteristics of rf-produced, high-density plasma with very small diameter”, *JPS Conf. Proc.,* Vol. 1, 2014, 015022-1~5.

[15]T. Nakagawa, Y. Sato, E. Tanaka, H. Iwaya, D. Kuwahara, S. Shinohara, “Study on Magnetized RF Discharge with Very Small-Diameter”, *Plasma Fusion Res*., Vol. 10, in press.

[16]S. Shinohara, T. Tanikawa, T. Hada, I. Funaki, H. Nishida, T. Matsuoka, F. Otsuka, K. P. Shamrai, T. S. Rudenko, T. Nakamura, A. Mishio, H. Ishii, N. Teshigahara, H. Fujitsuka, S. Waseda, “High-Density Helicon Plasma Sources: Basics and Application to Electrodeless Electric Propulsion”, *Trans. Fusion Sci. Technol.*, Vol. 63, 2014, pp.164-167.

[17]F. Otsuka, T. Hada, S. Shinohara, T. Tanikawa, and T. Matsuoka, “Numerical studies of Ponderomotive acceleration and ion cyclotron resonance: application to next generation electric thrusters”, *Plasma Fusion Res*., Vol. 8, 2013, pp. 2406012-1~14.

[18]F. Otsuka, T. Hada, S. Shinohara, T. Tanikawa, and T. Matuoka, “Numerical modeling of electrodeless electric thruster by ion cyclotron resonance/Ponderomotive acceleration”, *Plasma Fusion Res.*, Vol, 8, 2013, pp. 2406067-1~7.

[19]T. Nakamura, S. Ito, H. Nishida, S. Shinohara, I. Funaki, T. Tanikawa, T. Hada, “Thrust performance of high magnetic field permanent magnet type helicon plasma thruster”, 50th *AIAA Propul. Conf.*, 2014, AIAA2014-3474.